



# Density-dependent enhancement of methane oxidation activity and growth of *Methylocystis* sp. by a non-methanotrophic bacterium *Sphingopyxis* sp.



So-Yeon Jeong<sup>a</sup>, Kyung-Suk Cho<sup>a</sup>, Tae Gwan Kim<sup>a,b,\*</sup>

<sup>a</sup> Global Top 5 Program, Department of Environmental Science and Engineering, Ewha Womans University, 52, Ewhayeodae-gil, Seodaemun-gu, Seoul 120-750, Republic of Korea

<sup>b</sup> Department of Ecosystem Function, Bureau of Basic Ecological Research, National Institute of Ecology, 1210, Geumgang-ro, Maseo-myeon, Seocheon-gun, Chungcheongnam-do 325-813, Republic of Korea

## ARTICLE INFO

### Article history:

Received 17 June 2014

Received in revised form 11 September 2014

Accepted 23 September 2014

Available online 26 September 2014

### Keywords:

*Methylocystis*

*Sphingopyxis*

Population growth

Microbial interaction

Methanotrophic activity

## ABSTRACT

Methanotrophs are a biological resource as they degrade the greenhouse gas methane and various organic contaminants. Several non-methanotrophic bacteria have shown potential to stimulate growth of methanotrophs when co-cultured, and however, the ecology is largely unknown. Effects of *Sphingopyxis* sp. NM1 on methanotrophic activity and growth of *Methylocystis* sp. M6 were investigated in this study. M6 and NM1 were mixed at mixing ratios of 9:1, 1:1, and 1:9 (v/v), using cell suspensions of  $7.5 \times 10^{11}$  cells L<sup>-1</sup>. Methane oxidation of M6 was monitored, and M6 population was estimated using fluorescence *in situ* hybridization (FISH). Real-time PCR was applied to quantify rRNA and expression of transcripts for three enzymes involved in the methane oxidation pathway. NM1 had a positive effect on M6 growth at a 1:9 ratio ( $p < 0.05$ ), while no significant effects were observed at 9:1 and 1:1 ratios. NM1 enhanced the methane oxidation 1.34-fold at the 1:9 ratio. NM1 increased the population density and relative rRNA level of M6 by 2.4-fold and 5.4-fold at the 1:9 ratio, indicating that NM1 stimulated the population growth of M6. NM1 increased the relative transcriptional expression of all mRNA targets only at the 1:9 ratio. These results demonstrated that NM1 enhanced the methanotrophic activity and growth of M6, which was dependent on the proportion of NM1 present in the culture. This stimulation can be used as management and enhancement strategies for methanotrophic biotechnological processes.

© 2014 The Authors. Published by Elsevier B.V. This is an open access article under the CC BY-NC-ND license (<http://creativecommons.org/licenses/by-nc-nd/3.0/>).

## 1. Introduction

Methanotrophic bacteria utilize CH<sub>4</sub> as their sole carbon and energy source, and thus are important in the global carbon cycle [25]. They are highly diverse and found in a wide range of environments [9,25]. Most of the known methanotrophic bacteria belong to the *Alphaproteobacteria* and *Gammaproteobacteria*, and some *Verrucomicrobia* isolates are known to be methanotrophs [25]. They transform CH<sub>4</sub> to CO<sub>2</sub>, with methanol, formaldehyde and formate as intermediates [9]. In the field of biotechnology, methanotrophs are a valuable biological resource because they can degrade the greenhouse gas methane, and co-metabolize

various organic compounds [25,27]. Therefore, methanotrophs are used in environmental engineering systems to mitigate methane emission and to remove recalcitrant contaminants (e.g., trichloroethylene) [7,20,23].

Various abiotic and biotic factors can affect the growth and activity of methanotrophs [1,26,30]. Previous studies largely focused on abiotic factors such as oxygen, nutrients, moisture, and temperature, etc. to enhance methanotrophic activity [9,25]. However, recent studies have indicated that methanotrophs interact significantly with other bacteria in different ways. Stable isotope probing (SIP) revealed metabolic interaction between methanotrophs and non-methanotrophic bacteria in a natural environment [12]. Iguchi et al. [13] recently found that isolates of *Rhizobium*, *Sinorhizobium*, *Mesorhizobium*, *Xanthobacter*, and *Flavobacterium* enhanced the methanotrophic activity of *Methylovulum miyakonense* (belonging to *Gammaproteobacteria*), and that the *Rhizobium* isolate stimulated the methanotrophic activities of other *Gammaproteobacteria* methanotrophs belonging to

\* Corresponding author at: National Institute of Ecology, Department of Ecosystem Function, Bureau of Basic Ecological, 1210, Geumgang-ro, Maseo-myeon, Seocheon-gun, Chungcheongnam-do 325-813, Republic of Korea.  
Tel.: +82 41 950 5370; fax: +82 41 950 5953.

E-mail address: [niceguyktk@gmail.com](mailto:niceguyktk@gmail.com) (T.G. Kim).

*Methylococcaceae*, *Methylomonas*, and *Methylobacter* by producing an extracellular compound. Similarly, Stock et al. [26] reported that several heterotrophic bacterial isolates increased the biomass of co-cultures with methanotrophs. In addition, Ho et al. [10] reported that richness of heterotrophic bacteria was an important factor in stimulating methanotrophic activity. Microorganisms other than those isolates may also be able to enhance growth and/or activity of methanotrophs. These non-methanotrophic organisms could potentially be used as biological stimulators in methanotrophic engineering systems. To enhance methanotrophic systems using a biological stimulator, the interaction of the stimulator with methanotrophs should be elucidated. For instance, it should be determined if this type of biological stimulation is a density-dependent process.

We obtained a stable methanotrophic consortium from soil, which had been maintained with methane as sole carbon and energy for more than a year. We found that *Methylocystis* (belonging to *Alphaproteobacteria*) comprised 73% of the community, followed by *Sphingopyxis*, a common soil heterotrophic bacterium [25%] when examining the community using ribosomal tag pyrosequencing (unpublished data). Therefore, we hypothesized that *Sphingopyxis* interacts positively with *Methylocystis*. The main objectives of this study were to determine if *Sphingopyxis* enhances the methane oxidation of *Methylocystis*, if *Sphingopyxis* stimulates the population growth and/or activity (methane oxidation enzymes) of *Methylocystis*, and if this biological stimulation is a density-dependent process. To address these questions, *Methylocystis* and *Sphingopyxis* were mixed at different mixing ratios. Methane oxidation rate was calculated at each ratio. Population density and rRNA expression were quantified using FISH and real-time PCR. mRNA expression levels of genes involved in the methane oxidation pathway were also quantified.

## 2. Materials and methods

### 2.1. Organisms

*Methylocystis* sp. M6 and *Sphingopyxis* sp. NM1 were used in this study. The two bacteria originated from soil, but were not isolated from the same consortium. The obligate methanotroph M6 [15] was maintained in nitrate mineral salts (NMS) medium with 50,000 ppm methane as previously described by [16]. NMS medium contained  $\text{MgSO}_4 \cdot 7\text{H}_2\text{O}$   $1 \text{ g L}^{-1}$ ,  $\text{CaCl}_2 \cdot 2\text{H}_2\text{O}$   $0.134 \text{ g L}^{-1}$ ,  $\text{KNO}_3$   $1 \text{ g L}^{-1}$ ,  $\text{KH}_2\text{PO}_4$   $0.272 \text{ g L}^{-1}$ ,  $\text{Na}_2\text{HPO}_4 \cdot 12\text{H}_2\text{O}$   $0.717 \text{ g L}^{-1}$  [29].  $\text{CuSO}_4$  was added to a final concentration of  $30 \mu\text{M}$  for supporting the pMMO activity and growth of M6 [9,22]. NM1 was isolated from the *Methylocystis*- and *Sphingopyxis*-dominant methanotrophic consortium. The consortium was serially diluted using sterile 0.9% NaCl solution and spread on Difco™ R2A agar (BD Diagnostics, Sparks, MD, USA) plates. A pure colony of NM1 was obtained by subsequent transfers to new R2A agar plates more than three times, and maintained in R2A agar medium. To identify NM1, the 16S rRNA gene was amplified using the primer pair 341f (5'-CCTACGGGAGG-CAGCAG-3') and 907r (5'-CCCCGTCAATTCATTTGAGTTT-3'). The partial sequence of the 16S rRNA gene was compared with known DNA sequences using Basic Local Alignment Search Tool (BLAST) analysis (<http://blast.ncbi.nlm.nih.gov>). NM1 was identified as a *Sphingopyxis* sp. The sequence was deposited into the GenBank (<http://www.ncbi.nlm.nih.gov>) database under the accession number AB935326. When carbon source patterns were analyzed using BIOLOG™ Ecoplates (Biolog, Hayward, USA), NM1 was found to utilize D-galacturonic acid, D-mannitol, D-xylose, and pyruvic acid methyl ester. M6 and NM1 have been deposited in the Korean Collection for Type Cultures (<http://kctc.kribb.re.kr>) (World Data Center for Microorganisms, WDCM597) under the collection numbers KCTC 11519 and KCTC 32429, respectively.

### 2.2. Transmission electron microscopy

Bacterial cells were prefixed for 2 h in 0.1 M phosphate-buffered saline (PBS; pH 7.4) with 2.5% glutaraldehyde, and washed three times with PBS. Then, cells were fixed for 1 h in 1% osmium tetroxide, and washed with PBS. Dehydration was performed for 10 min each in 60%, 70%, 80%, 90%, and 95% ethanol, and then dehydrated twice for 10 min in 100% ethanol. Infiltration was conducted twice for 15 min with propylene oxide and cells were embedded with Epon-812. Appropriate areas of interest were selected from approximately  $1 \mu\text{m}$ -thick sections stained with toluidine blue. Ultra-thin sections (60–70 nm) were cut using an ultramicrotome (Richert–Jung, Fresno, CA, USA) and diamond knife. Thin sections were stained with 1–2% aqueous uranyl acetate, followed by 1% lead citrate. Stained sections were observed and photographed using a H-7650 transmission electron microscopic system (Hitachi, Tokyo, Japan). Cell masses of M6 and NM1 were estimated from TEM micrographs as described by [19]. Length and diameters were measured using ImageJ version 1.47 (<http://imagej.nih.gov/ij/>) ( $n=20$ ). Cell volume was calculated by the following equation:  $V = [(w^2 \times \pi/4) \times (l - w)] + (\pi \times w^3/6)$ , where  $V$  is the cell volume,  $w$  is the diameter and  $l$  is the length. Cell mass was calculated by the following equation:  $M = 435 \times V^{0.86}$ , where  $M$  is the mass ( $10^{-15}$  g).

### 2.3. Co-culture experiments

We confirmed that NM1 does not have methanotrophic activity (data not shown). M6 was cultivated in NMS medium with 50,000 ppm methane. NM1 was grown in R2A broth at  $30^\circ\text{C}$  with an agitation of 150 rpm for two days. After harvesting cells from each culture, they were washed twice with NMS by centrifugation at  $9000 \times g$  for 10 min and re-suspended in NMS. Cells were counted directly using a hemacytometer and transmission light microscope and then adjusted to a final concentration of  $7.5 \times 10^{11}$  cells  $\text{L}^{-1}$ . M6 was mixed with NM1 at ratios of 1:9, 1:1, and 9:1 (v/v, M6:NM1). As a control at each ratio, fresh NMS medium was added instead of NM1. 10 mL cell mixtures were placed in 120 mL serum bottles ( $n=5$ ). These bottles were sealed with a butyl-rubber stopper and parafilm. Methane (99.9%, Seoul special gas, Seoul, Korea) was spiked to a final concentration of 50,000 ppm. Serum bottles were incubated at  $30^\circ\text{C}$  with an agitation of 150 rpm. When methane concentration was below 1000 ppm, the serum bottles were aerated on a clean bench, and methane was spiked again into the bottles. Each of the bottles was spiked with methane three times. The co-culture experiments were done within a week. At the end of the experiment, cells were harvested from 1 mL of each culture by centrifugation at  $13,000 \times g$  for 10 min. Harvested cells were frozen at  $-70^\circ\text{C}$  prior to use.

### 2.4. Gas analysis

Methane concentration was monitored using gas chromatograph (GC, 6850N, Agilent Technologies, Santa Clara, CA, USA) equipped with a wax column ( $30 \text{ m} \times 0.32 \text{ mm} \times 0.25 \mu\text{m}$ , Supelco, Bellefonte, PA, USA) and a flame ionization detector. The oven, injector, and detector temperatures were set at 100, 230, and  $230^\circ\text{C}$ , respectively.

### 2.5. Fluorescence in situ hybridization

M6 cells were enumerated using fluorescence *in situ* hybridization (FISH). FISH is a useful tool for direct counting and visualization of bacterial cells [5,21]. The sample was hybridized with a TAMRA-linked probe (5'-CGTTGGCGAAACGCCCTT-3') [3]. Cells were fixed for 2 h in 500  $\mu\text{L}$  of phosphate-buffered saline (PBS, pH 7.4) with 4% paraformaldehyde, and washed twice with

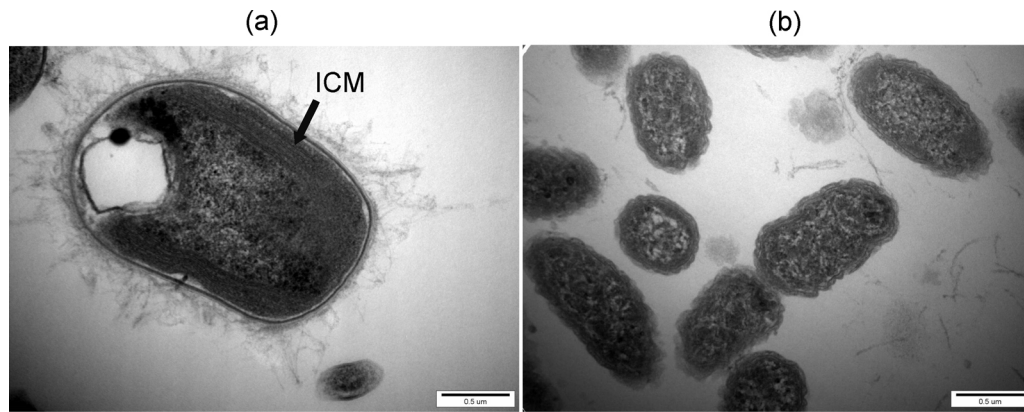


Fig. 1. Micrographs of *Methylocystis* sp. M6 (a) and *Spingopyxis* sp. NM1 (b) obtained by transmission electron microscopy. Scale bars represent 0.5  $\mu\text{m}$ .

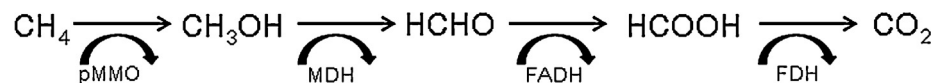
PBS. Pellets were re-suspended in 0.5 mL of ethanol:PBS [1:1]. A 2  $\mu\text{L}$  aliquot of the cell suspension was placed on slide glass (10 reaction wells,  $\varnothing$ 7 mm, Marienfeld, Germany) and then air-dried. Dehydration was performed for 3 min each in 50%, 80%, and 100% ethanol, and then samples were air-dried. Cells were pre-hybridized for 30 min at 50  $^{\circ}\text{C}$  in hybridization buffer (0.9 M NaCl, 20 mM Tris-HCl, and 0.01% SDS). Hybridization was performed for 2 h in hybridization buffer containing 5 ng/ $\mu\text{L}$  of the probe. Cells were briefly washed with washing buffer, and then immersed for 20 min in washing buffer (20 mM Tris-HCl, 0.01% SDS and 0.9 M NaCl) at 50  $^{\circ}\text{C}$ . Cells were then rinsed twice with ultrapure water, air-dried, and stained with 2  $\mu\text{M}$  4,6-diamidino-2-phenylindole (DAPI) for 10 min at room temperature in the dark. Cells were washed with ultrapure water and after allowing them to air-dry at room temperature, cover glasses were mounted with a drop of

USA) according to the manufacturer's recommendations. RNA was eluted in 30  $\mu\text{L}$  of the elution buffer and quantified using an ASP-2680 spectrophotometer (ACTGene, Piscataway, NJ, USA).

RNA was reverse-transcribed using the Omniscript RT kit (Qiagen) according to the manufacturer's recommendations. Reverse transcription reactions were performed in 20- $\mu\text{L}$  volumes. The reaction mixture consisted of 1  $\mu\text{L}$  of 1  $\times$  buffer RT, 2  $\mu\text{L}$  of dNTP, random hexamer at 50  $\mu\text{M}$ , 10 U of RNase inhibitor, 1  $\mu\text{L}$  of Omniscript RT, and 10  $\mu\text{L}$  of template RNA.

### 2.7. Real-time PCR

Methane oxidation is mediated by several enzymes as shown in the following pathway.



Mowiol on the slide glass. Cells were observed using an Axiovert 200 microscopic system (Carl Zeiss, Göttingen, Germany). TAMRA fluorescence was detected using the 546 excitation and LP 590 emission filter set. DAPI fluorescence was detected using the 365 excitation and BP 445 emission filter set. Twenty focal areas were selected randomly from a well of the slide glass and M6 cells were counted directly.

### 2.6. RNA extraction and cDNA conversion

RNA was extracted using TRIzol<sup>®</sup> Reagent (Invitrogen, Carlsbad, CA, USA). First, 0.75 mL of TRIzol<sup>®</sup> Reagent were added to tubes containing 0.25 mL of sample. Tubes were mixed well and incubated at room temperature for 5 min. For phase separation of sample, 0.15 mL of chloroform was added to the tubes containing samples and the tubes were shaken by hand for 15 s. Tubes were then incubated for 2 min at room temperature and centrifuged at 12,000  $\times g$  for 15 min at 4  $^{\circ}\text{C}$ . Top aqueous layer was transferred to a new tube, and 0.375 mL of 100% isopropanol was added. After incubation at room temperature for 10 min, tubes were centrifuged at 12,000  $\times g$  for 10 min at 4  $^{\circ}\text{C}$ . Pellets were washed with 0.75 mL of 75% ethanol, and then centrifuged at 7500  $\times g$  for 5 min at 4  $^{\circ}\text{C}$ . RNA pellets were air-dried and re-suspended in 50  $\mu\text{L}$  of RNase-free water, and then incubated in a water bath at 60  $^{\circ}\text{C}$  for 10 min. Five micro litre of 10  $\times$  DNase I buffer (Ambion, Austin, TX, USA) and 1  $\mu\text{L}$  of DNase I (Ambion) were added to tubes containing 50  $\mu\text{L}$  of RNA sample. Mixtures were incubated in a water bath at 37  $^{\circ}\text{C}$  for 30 min. RNA was purified using the RNeasy Mini Kit (Qiagen, Valencia, CA,

where pMMO is the particulate methane monooxygenase, MDH is the methanol dehydrogenase, FADH is the formaldehyde dehydrogenase, and FDH is the formate dehydrogenase [9,25]. rRNA as well as transcript levels of pMMO, MDH, and FADH genes were quantified using an Applied Biosystems 7300 real-time PCR system (Applied Biosystems, Carlsbad, CA, USA). Multiple forward and reverse primer sets were designed for each gene, based on the rRNA (accession number: [GQ255542](http://www.ncbi.nlm.nih.gov/nucl/1255542)), pMMO (AB936294), MDH (AB936295), and FADH (AB936293) gene sequences using Primer-BLAST (<http://www.ncbi.nlm.nih.gov/tools/primer-blast/>). Designed sets were evaluated *in silico* by computing coverage of the nucleotide sequences (forward and reverse primers) against sequences of *Sphingomonadaceae* in the NCBI database. Primer sets were selected for each gene according to the specificity. The following primer sets were used in this study: (1) 16S-F (5'-CGGAATCACTGGGCGTAAA-3') and 16S-R (5'-GACTCGAGACCTCCAGTATCA-3') for rRNA, (2) pmoA-F (5'-TTCTGGTGGGTGAATTCGCCTT-3') and pmoA-R (5'-AAGCAGGATCACGTCAGCCAGAT-3') for pMMO, (3) MDH-F (5'-TCGACGACACCGTCAATGTGTTC-3') and MDH-R (5'-TGGTTCACGCCAAGAAAGAACAGC-3') for MDH, and (4) FADH-F (5'-CGATCGACATTCGGATATTCGCC-3') and FADH-R (5'-TCGTGGAAATGATAGCGCAGTG-3') for FADH.

RT-PCR reactions were performed in 25  $\mu\text{L}$  reaction volumes. The reaction mixture consisted of 12.5  $\mu\text{L}$  of PCR premix (Qiagen), 0.5  $\mu\text{L}$  of forward primer (10  $\mu\text{M}$ ), 0.5  $\mu\text{L}$  of reverse primer (10  $\mu\text{M}$ ), and 2  $\mu\text{L}$  of template cDNA. Control reactions contained

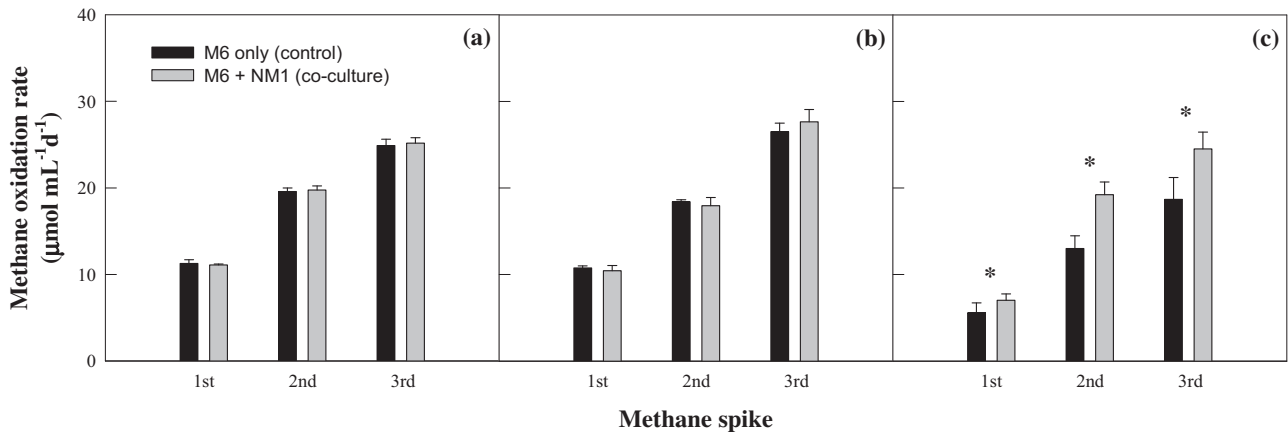


**Fig. 2.** Methane oxidation rates of co-cultures. *Methylocystis* sp. M6 and *Sphingopyxis* sp. NM1 were mixed at 9:1 (a), 1:1 (b), and 1:9 (c) ( $n=5$ ). The symbol \* indicates a significant difference at  $p < 0.05$ .

the same mixtures but with 2  $\mu\text{L}$  of ultrapure water replacing the cDNA template. PCR was initiated at 95  $^{\circ}\text{C}$  for 15 min, followed by 40 cycles of 94  $^{\circ}\text{C}$  for 15 s and 60  $^{\circ}\text{C}$  for 1 min.

Relative rRNA and mRNA expressions in M6 were estimated, based on intervals of Ct values in the treatment and control samples. Relative expression (RE) was calculated as  $\text{RE} = \frac{2^{-(\text{treatment Ct} - \text{control Ct})}}{(\text{Pt}/\text{Pc})}$ , where Ct is the threshold cycle number, Pt is the M6 population of the treatment, and Pc is the M6 population of the control.

### 3. Results and discussion

#### 3.1. Morphological characteristics of the two organisms

TEM micrographs of M6 and NM1 are shown in Fig. 1. M6 is  $1.89 \pm 0.27 \mu\text{m}$  in length and  $1.12 \pm 0.20 \mu\text{m}$  in diameter, and NM1 is  $1.01 \pm 0.23 \mu\text{m}$  in length and  $0.57 \pm 0.06 \mu\text{m}$  in diameter. The cell masses of M6 and NM1 were estimated to be  $612.1 \times 10^{-15}$  and  $114.7 \times 10^{-15}$  g, respectively. Cell mass of M6 is 5.3-fold greater than that of NM1. M6 is cocci-rod in shape and has well developed intracytoplasmic membranes (ICM). ICM has been observed in other methanotrophs; it is hypothesized that these membranes are related to the enzymatic process of methane oxidation [6,18,24]. NM1 has a rod-like shape and a multilayer cell wall with no flagella. Lee et al. [17] reported that *Sphingopyxis* sp. Gsoil 250T is

motile and rod-shaped (0.2–0.3 mm in diameter and 1.0–1.2 mm in length) with a single flagellum.

#### 3.2. Effects of NM1 on methane oxidation activity of M6

NM1 showed no negative effect on methane oxidation (Fig. 2). Methane oxidation rate (MOR) of M6 increased with the number of methane spikes in all cultures, regardless of whether NM1 was added or not ( $p < 0.05$ ). MOR increased 2-fold with the second spike and 3-fold with the third spike. This increase was likely due to the population growth of M6 over time, because methane oxidation is dependent on the biomass of methanotrophs [14]. Addition of NM1 significantly increased the MOR at the 1:9 ratio of M6:NM1 ( $p < 0.05$ ), but not at the other two ratios ( $p > 0.05$ ). Thus, NM1 could enhance the methane oxidation when it was more populated than M6.

#### 3.3. Effects of NM1 on population growth of M6

FISH results indicated that the presence of NM1 appeared to stimulate the population growth of M6 (Fig. 3). The effect of NM1 was statistically significant at the 1:9 ratio ( $p < 0.05$ ) while not significant at the 9:1 and 1:1 ratios ( $p > 0.05$ ). Ribosomal RNA is essential for protein synthesis in organisms as a component of the ribosome [2], and its synthesis rate can reflect the cell growth rate [8,28]. Relative rRNA levels (treatment to control) were estimated to determine if NM1 induces cell growth of M6 (Fig. 4). The added NM1 increased the relative rRNA level at all ratios; however, the effect was only significant at the 1:9 ratio of M6:NM1 ( $p < 0.05$ ), consistent with the population results. The relative rRNA levels were  $1.05 \pm 0.26$ ,  $1.03 \pm 0.10$  and  $5.39 \pm 1.44$  at the 9:1, 1:1 and 1:9 ratios of M6:NM1, respectively. Both results indicated that NM1 stimulated the population growth of M6 in a density-dependent manner. This population increase is one mechanism by which NM1 can increase MOR because methane oxidation activity is positively correlated with the cell number of methanotrophs in a system [4,13,14].

#### 3.4. Effects of NM1 on transcriptional expression of pMMO, MDH, and FADH

A previous study showed that non-methanotrophs stimulated methanotrophic growth in the co-cultures [13]. However, it is not known whether this is due to induction of methane oxidation pathways or not. We therefore measured transcriptional expression of pMMO, MDH, and FADH, which are involved in methane oxidation.

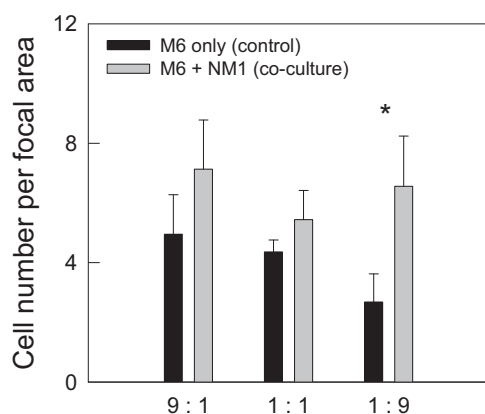


**Fig. 3.** Populations of *Methylocystis* sp. M6 per focal area. *Methylocystis* sp. M6 and *Sphingopyxis* sp. NM1 were mixed at 9:1, 1:1, and 1:9 ratios ( $n=5$ ). For population measurement, 20 focal spots were randomly selected and M6 cells were directly counted. The symbol \* indicates a significant difference at  $p < 0.05$ .



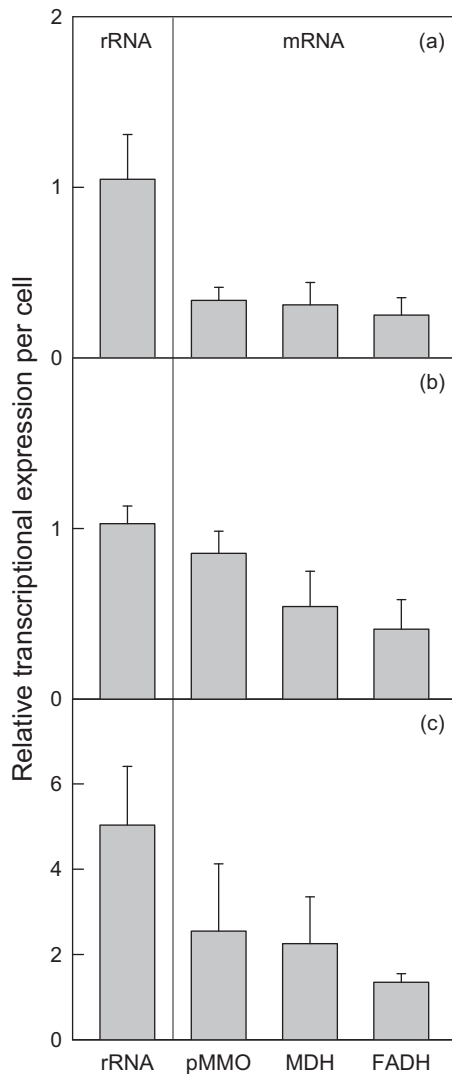


**Fig. 4.** Relative transcriptional expression levels of ribosomal RNA and the particulate methane monooxygenase, methanol dehydrogenase, and formaldehyde dehydrogenase genes (treatment to control). *Methylocystis* sp. M6 to *Sphingopyxis* sp. NM1 were mixed at 9:1 (a), 1:1 (b), and 1:9 (c) ratios ( $n=5$ ).

Fig. 4 shows the relative mRNA expression levels of the pMMO, MDH and FADH genes. The relative mRNA expression levels of pMMO at the 9:1, 1:1, and 1:9 ratios of M6:NM1 were  $0.34 \pm 0.08$ ,  $0.85 \pm 0.13$ , and  $2.67 \pm 1.31$ , those of MDH were  $0.31 \pm 0.13$ ,  $0.54 \pm 0.21$ , and  $2.40 \pm 0.94$ , and those of FADH were  $0.25 \pm 0.10$ ,  $0.41 \pm 0.17$ , and  $1.26 \pm 0.24$ , respectively. The relative expression levels of all genes were less than 0.5 at the 9:1 ratio of M6:NM1 and less than 1 at the 1:1 ratio. Interestingly, relative expression ratio was at least 1.3-fold higher at the 1:9 ratio of M6:NM1.

These results indicated that NM1 enhanced the transcriptional expression of the genes involved in methane oxidation when NM1 was more abundant than M6, consistent with the population and methane oxidation rate results. Relative expression of FADH was about 2-fold lower than the expression levels of the pMMO and MDH genes. We speculate that some of the formaldehyde produced was used for biosynthesis because formaldehyde has a central role as an intermediate in catabolism and anabolism [9]. Increased transcriptional expression of these genes was likely responsible for the increased oxidation rate measured at the 1:9

ratio of M6:NM1. Similarly, [11] reported that the amount of mRNA copies was correlated with the activity in the reactor.

We demonstrated that NM1 concurrently enhanced the population growth of M6 and the expression of the methane-oxidation genes in a density-dependent manner. The two types of bacterial cells were mixed on the basis of cell number. Because the mass of NM1 cells is 5.7-fold less than that of M6, the mass-ratio of NM1 to M6 was estimated to be 0.02, 0.19, and 1.68 at the 9:1, 1:1, and 1:9 ratios of M6:NM1. NM1 only had significant effects on the activity and growth of M6 at the 1:9 ratio of M6:NM1, indicating that NM1 had a significant effect on M6 only when it was present at higher mass than M6. Previous studies have shown that a few vitamins and organic acids can enhance methanotrophic growth [31]. For instance, [13] reported that cobalamin (vitamin B<sub>12</sub>) produced by *Rhizobium* stimulated the growth and activity of several methanotrophs, including *Methylomonas* and *Methylovulum*. Xing et al. [31] reported that riboflavin and organic acids (maleate, succinate, malate, and citrate) induced the population growth of *Methylosinus*. Thus, we hypothesize that extracellular substances from NM1 enhanced the population growth of M6 as well as the expression of the methane-oxidation enzymes in M6. Further investigations of the metabolic interactions between these two organisms are warranted. Our results also imply that methane oxidizers may commonly interact with other organisms in natural environments.

#### 4. Conclusions

This is the first study to report that the non-methanotrophic bacterium *Sphingopyxis* enhances the activity of the type II methanotroph *Methylocystis*. We demonstrated that NM1 enhanced the population growth of M6 as well as the expression of the genes involved in the methane oxidation pathway in a density-dependent manner. These results can be used to develop and guide management and enhancement strategies for methanotrophic biotechnological processes. For instance, this stimulation can be used for accelerating start-up in methanotrophic systems.

#### Acknowledgements

This research was supported by the Basic Science Research Program through the National Research Foundation of Korea (NRF) funded by the Ministry of Science (2012R1A2A2A03046724) and by the Ministry of Education (2013R1A1A2061015).

#### References

- [1] S. Ait-Benichou, L.B. Jugnia, C.W. Greer, A.R. Cabral, Methanotrophs and methanotrophic activity in engineered landfill biocovers, *Waste Manage.* 29 (2009) 2509–2517.
- [2] A.E. Dahlberg, The functional role of ribosomal RNA in protein synthesis, *Cell* 57 (1989) 525–529.
- [3] S.N. Dedysh, P.F. Dunfield, M. Derakshani, S. Stubner, J. Heyer, W. Liesack, Differential detection of type II methanotrophic bacteria in acidic peatlands using newly developed 16 S rRNA-targeted fluorescent oligonucleotide probes, *EFEMS Microbiol. Ecol.* 43 (2003) 299–308.
- [4] D. Dianou, K. Adachi, Characterization of methanotrophic bacteria isolated from a subtropical paddy field, *FEMS Microbiol. Lett.* 173 (1999) 163–173.
- [5] G. Eller, S. Stubner, P. Frenzel, Group-specific 16 S rRNA targeted probes for the detection of type I and type II methanotrophs by fluorescence *in situ* hybridisation, *FEMS Microbiol. Lett.* 198 (2001) 91–97.
- [6] B.T. Eshinimaev, K. Medvedkova, V. Khmelina, N. Suzina, G. Osipov, A. Lysenko, Y.A. Trotsenko, New thermophilic methanotrophs of the genus *Methylocaldum*, *Microbiology* 73 (2004) 448–456.
- [7] J. Gebert, A. Gröngroft, Performance of a passively vented field-scale biofilter for the microbial oxidation of landfill methane, *Waste Manage.* 26 (2006) 399–407.
- [8] J.D. Gralla, *Escherichia coli* ribosomal RNA transcription: regulatory roles for ppGpp NTPs, architectural proteins and a polymerase-binding protein, *Mol. Microbiol.* 55 (2005) 973–977.

- [9] R.S. Hanson, T.E. Hanson, Methanotrophic bacteria, *Microbiol. Mol. Biol. R. 60* (1996) 439–471.
- [10] A. Ho, K. de Roy, O. Thas, J. De Neve, S. Hoefman, P. Vandamme, K. Heylen, N. Boon, The more, the merrier: heterotroph richness stimulates methanotrophic activity, *ISME J.* (2014) .
- [11] Y. Huang, W. Zong, X. Yan, R. Wang, C.L. Hemme, J. Zhou, Z. Zhou, Succession of the bacterial community and dynamics of hydrogen producers in a hydrogen-producing bioreactor, *Appl. Environ. Microbiol.* 76 (2010) 3387–3390.
- [12] E. Hutchens, S. Radajewski, M.G. Dumont, I.R. McDonald, J.C. Murrell, Analysis of methanotrophic bacteria in Movile Cave by stable isotope probing, *Environ. Microbiol.* 6 (2004) 111–120.
- [13] H. Iguchi, H. Yurimoto, Y. Sakai, Stimulation of methanotrophic growth in cocultures by cobalamin excreted by rhizobia, *Appl. Environ. Microbiol.* 77 (2011) 8509–8515.
- [14] T.G. Kim, T. Yi, J. Yun, H.W. Ryu, K.-S. CHO, Biodegradation capacity utilization as a new index for evaluating biodegradation rate of methane, *J. Microbiol. Biotechnol.* 23 (2013) 715–718.
- [15] E.H. Lee, K.E. Moon, H.W. Ryu, Characterization of methane oxidation by a methanotroph isolated from a landfill cover soil, South Korea, *J. Microbiol. Biotechnol.* 21 (2011) 753–756.
- [16] E.H. Lee, H. Park, K.-S. Cho, Characterization of methane, benzene and toluene-oxidizing consortia enriched from landfill and riparian wetland soils, *J. Hazard. Mater.* 184 (2010) 313–320.
- [17] M. Lee, L.N. Ten, H.-W. Lee, H.W. Oh, W.-T. Im, S.-T. Lee, *Sphingopyxis ginsengisoli* sp. nov., isolated from soil of a ginseng field in South Korea, *Int. J. Syst. Evol. Micr.* 58 (2008) 2342–2347.
- [18] C.D. Little, A.V. Palumbo, S.E. Herbes, M.E. Lidstrom, R.L. Tyndall, P.J. Gilmer, Trichloroethylene biodegradation by a methane-oxidizing bacterium, *Appl. Environ. Microbiol.* 54 (1988) 951–956.
- [19] M. Loferer-Krößbacher, J. Klima, R. Psenner, Determination of bacterial cell dry mass by transmission electron microscopy and densitometric image analysis, *Appl. Environ. Microbiol.* 64 (1998) 688–694.
- [20] M.J. McFarland, C.M. Vogel, J.C. Spain, Methanotrophic cometabolism of trichloroethylene (TCE) in a two stage bioreactor system, *Water Res.* 26 (1992) 259–265.
- [21] A. Moter, U.B. Göbel, Fluorescence *in situ* hybridization (FISH) for direct visualization of microorganisms, *J. Microbiol. Meth.* 41 (2000) 85–112.
- [22] S.D. Prior, H. Dalton, The effect of copper ions on membrane content and methane monooxygenase activity in methanol-grown cells of *Methylococcus capsulatus* (bath), *J. Gen. Microbiol.* 131 (1985) 155–163.
- [23] J. Rocha-Rios, S. Bordel, S. Hernández, S. Revah, Methane degradation in two-phase partition bioreactors, *Chem. Eng. J.* 152 (2009) 289–292.
- [24] D. Scott, J. Brannan, I. Higgins, The effect of growth conditions on intracytoplasmic membranes and methane mono-oxygenase activities in *Methylosinus trichosporium OB3b*, *Microbiology* 125 (1981) 63–72.
- [25] J.D. Semrau, A.A. DiSpirito, S. Yoon, Methanotrophs and copper, *FEMS Microbiol. Rev.* 34 (2010) 496–531.
- [26] M. Stock, S. Hoefman, F.M. Kerckhof, N. Boon, P. De Vos, B. De Baets, K. Heylen, W. Waegeman, Exploration and prediction of interactions between methanotrophs and heterotrophs, *Res. Microbiol.* 164 (2013) 1045–1054.
- [27] K.N. Takeuchi, H. Iwamoto, H. Nirei, T. Kusuda, O. Kazaoka, K. Furuya, Distribution of methanotrophs in trichloroethylene-contaminated aquifers in a natural gas field, *Geomicrobiol. J.* 18 (2001) 387–399.
- [28] R. Wagner, The regulation of ribosomal RNA synthesis and bacterial cell growth, *Arch. Microbiol.* 161 (1994) 100–109.
- [29] R. Whittenbury, K. Phillips, J. Wilkinson, Enrichment, isolation and some properties of methane-utilizing bacteria, *Microbiology* 61 (1970) 205–218.
- [30] J.H. Wilshusen, J.P. Hettiaratchi, A. De Visscher, R. Saint-Fort, Methane oxidation and formation of EPS in compost: effect of oxygen concentration, *Environ. Pollut.* 129 (2004) 305–314.
- [31] X.-H. Xing, H. Wu, M.-F. Luo, B.-P. Wang, Effects of organic chemicals on growth of *Methylosinus trichosporium* OB3b, *Biochem. Eng. J.* 31 (2006) 113–117.